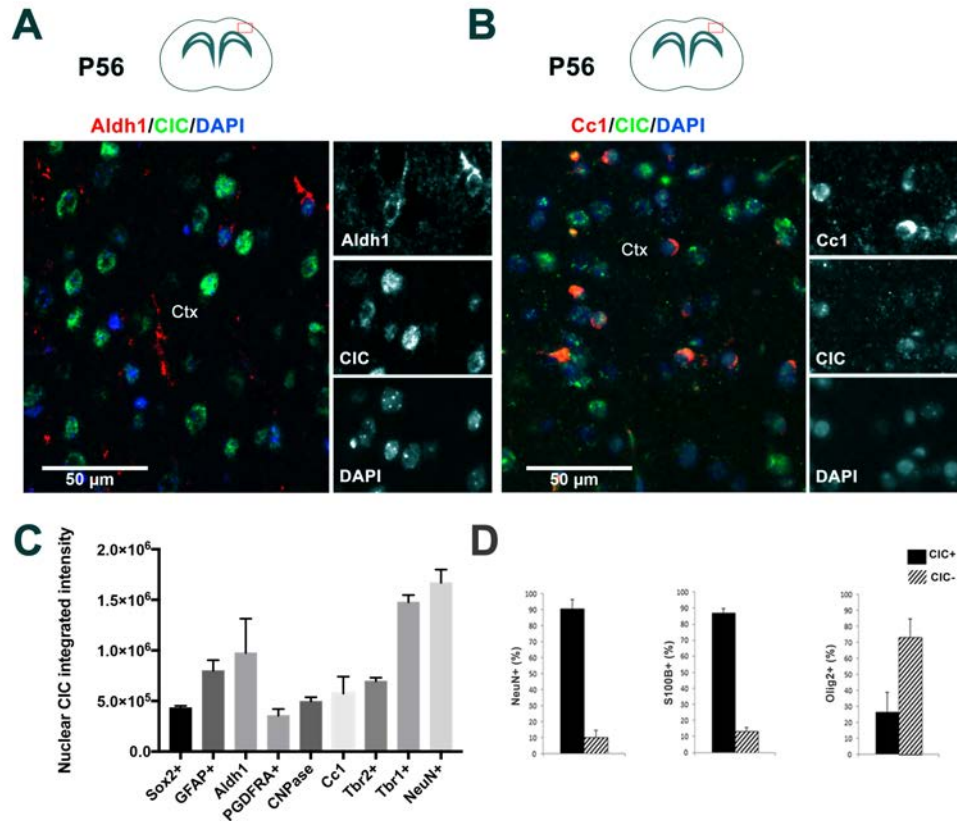# SUPPLEMENTAL DATA

SUPPLEMENTARY FIGURES (S1-S5)

Figure S1: CIC expression pattern in mammalian neural lineages. CIC expression in astrocytes labeled by Aldh1 antibody (A) and mature oligodendrocytes labeled by Cc1 antibody (B). (C) Bar graph showing Cic protein expression using immunostaining of mouse brain tissue. (D) Percentages of NeuN+ (neurons), S100B+ (astrocytes) and Olig2+ (oligodendrocytes) having CIC present or absent. Bars indicate mean±SD. Ctx-Cortex.
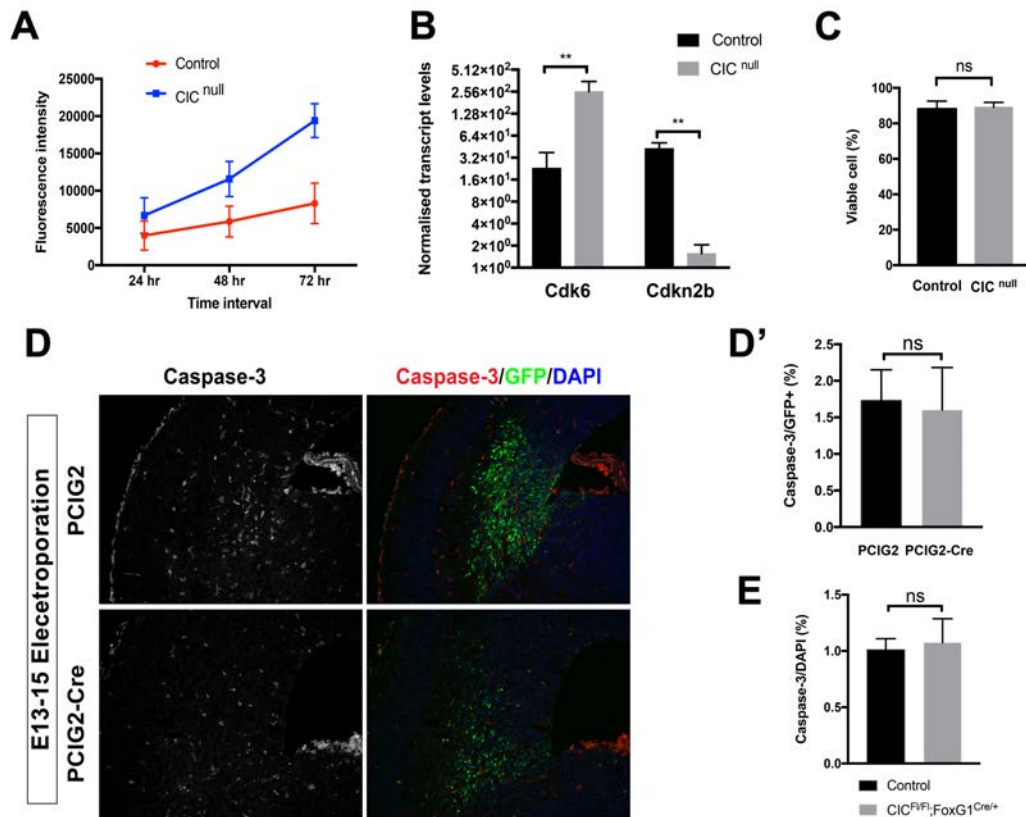
Figure S2: CIC loss affects proliferation but not apoptosis. (A) Alamar blue assay showing Cic loss induces higher cell proliferation rates at 24 hrs, 48 hrs and 72 hrs after seeding NSCs at equivalent density. (B) nanoString analysis of Cic null cells and control cell mRNA showing upregulation of *Cdk6* transcripts and downregulation of *P15INK* transcripts by Cic loss. (C) Trypan blue assay shows no difference in the viability of Cic null and control cells. (D) Cleaved Caspase-3 immunostaining shows no difference in the apoptotic cell numbers within GFP+ cells between Cic null and control cells. (E) Cleaved Caspase-3 immunostaining shows no difference in the apoptotic cell numbers within GFP+ cells between $Cic^{Fl/Fl};Foxg1^{Cre/+}$ and control brains. Bars indicate mean±SD. ns – not significant, ** $p < 0.01$.
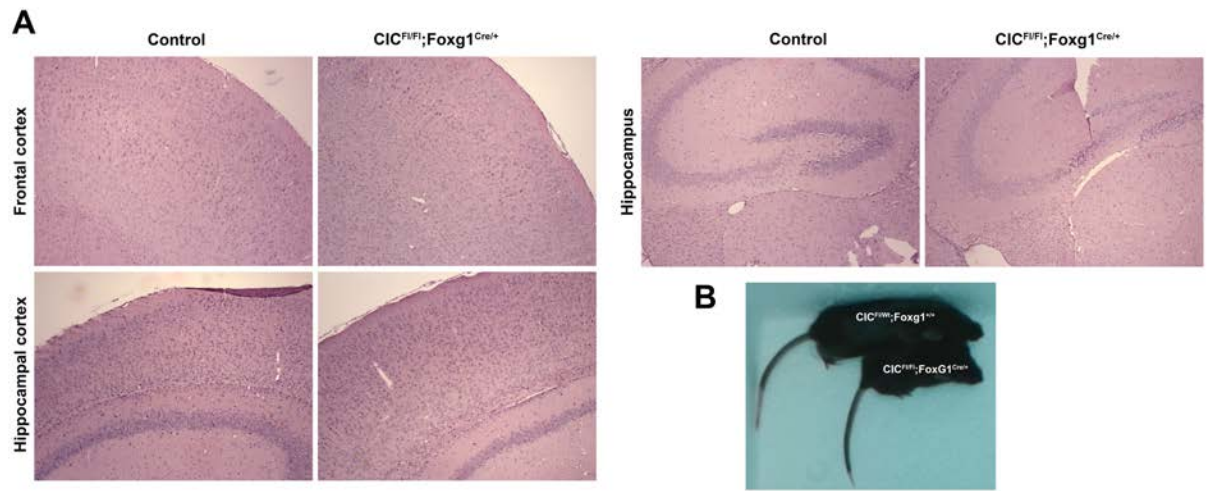
Figure S3: Additional phenotype of mice with forebrain *Cic* deletion. (A) Representative images showing histological examination of different areas of mouse brain at P21 revealing normal brain architecture in mice with *Cic* deletion in telencephalon. (B) At P21 the overall size of mice with *Cic* deletion in telencephalon showing strikingly smaller than the mice with intact *Cic*.
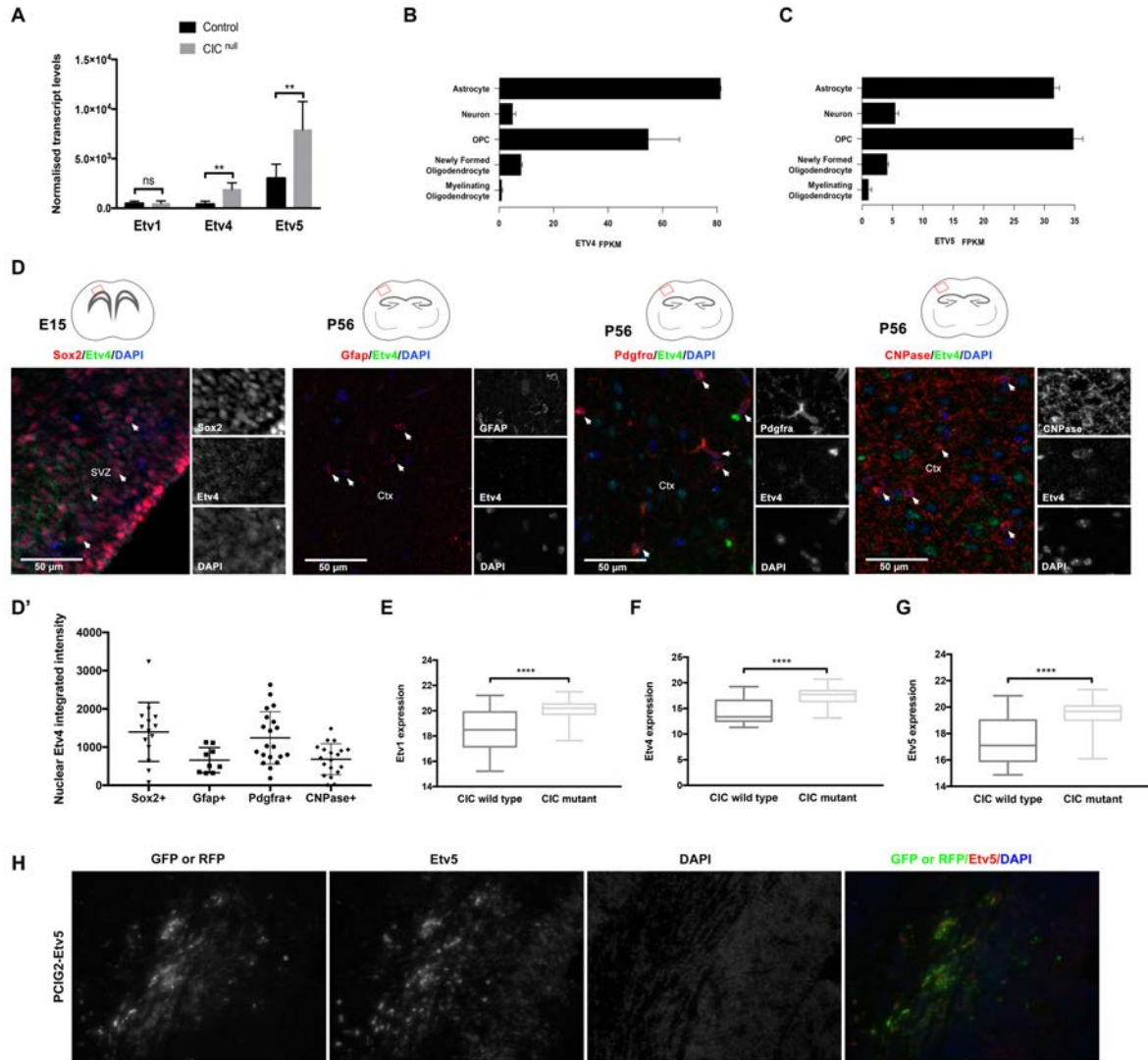
Figure S4: Inverse relationship of Ets factors with Cic levels. (A) Transcript levels of *Etv1*, *Etv4* and *Etv5* after 10 days of differentiation of mNSCs. (B) Our data is consistent with Barres lab RNAseq data showing high expression of *Etv4* and *Etv5* transcripts in OPCs and astrocytes (Suppl Ref 1). (C) Etv4 protein expression in mouse brain cortical sections across different neural lineages using specific neural lineage markers. (D,D') Quantification of the Etv4 protein expression across neural lineages. (G) Oligodendroglioma patient cohort (TCGA Low Grade Glioma data set) *ETV1*, *ETV4* and *ETV5* transcripts levels between *CIC*-mutant and -wildtype patients indicates higher expression of *ETS* factors in *CIC*-mutant low grade gliomas compared to *CIC*-wildtype low grade gliomas when controlled for *IDH* mutation status. (H) Immunostaining for Etv5 protein confirms that *in-utero* electroporation of *Etv5* construct into mouse forebrain results in localized increased expression of Etv5. SVZ – Sub-ventricular zone, Ctx- Cortex. ns – not significant, ** p<0.01, **** p<0.0001.
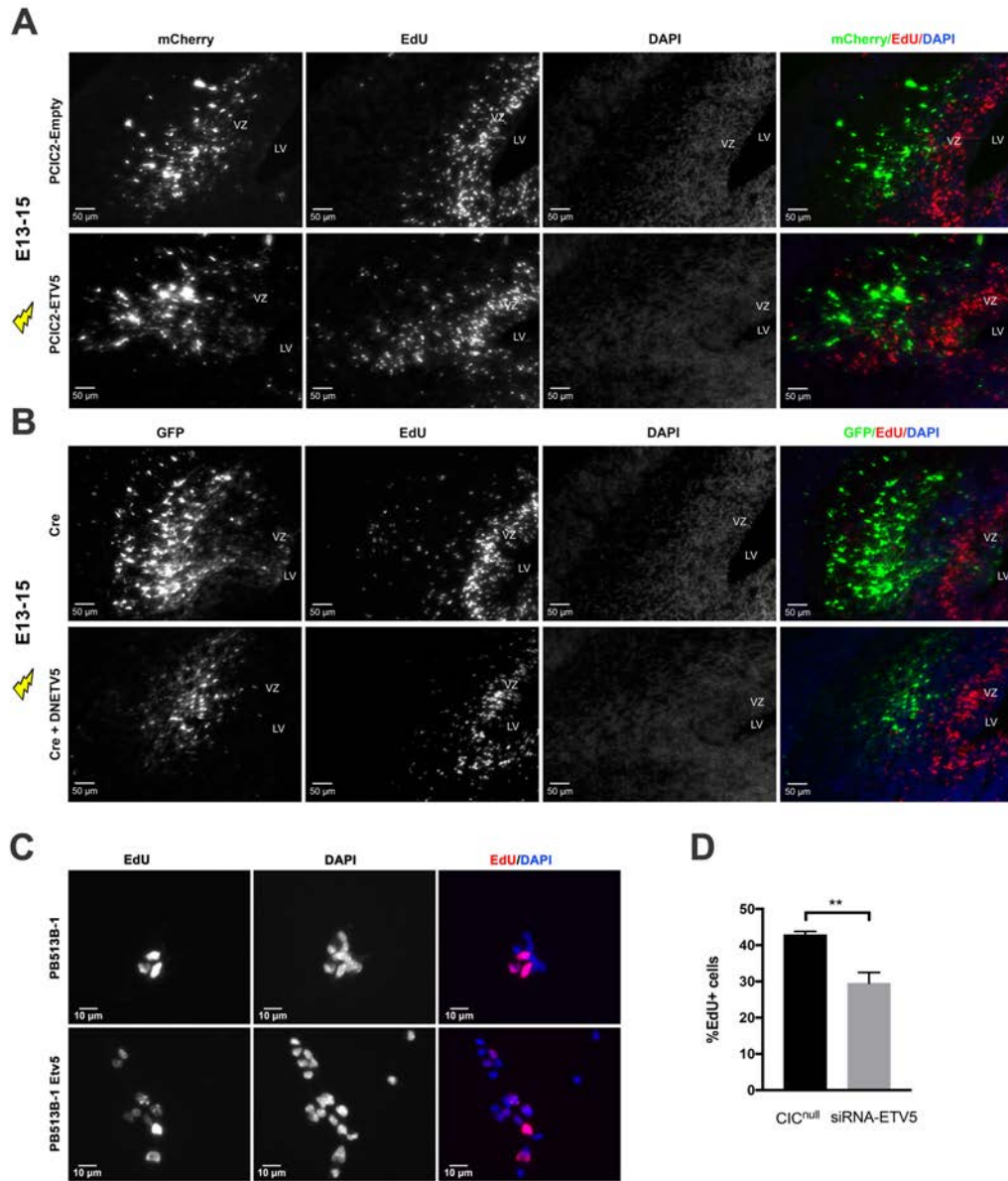
Figure S5: The proliferative phenotype induced by CIC loss is Etv5-dependent. (A) Representative images showing Etv5 overexpression increases the percentage of cycling EdU+ cells in electroporated mice. (B) Etv5 blockade rescues the high proliferation induced by CIC loss. (C) Etv5 overexpression increases percentage of EdU+ cells in cultured mNSCs. Quantification of percentage of EdU+ cells with siRNA knockdown of ETV5 (D). VZ – Ventricular zone, LV – Lateral ventricle. ** $p<0.01$.
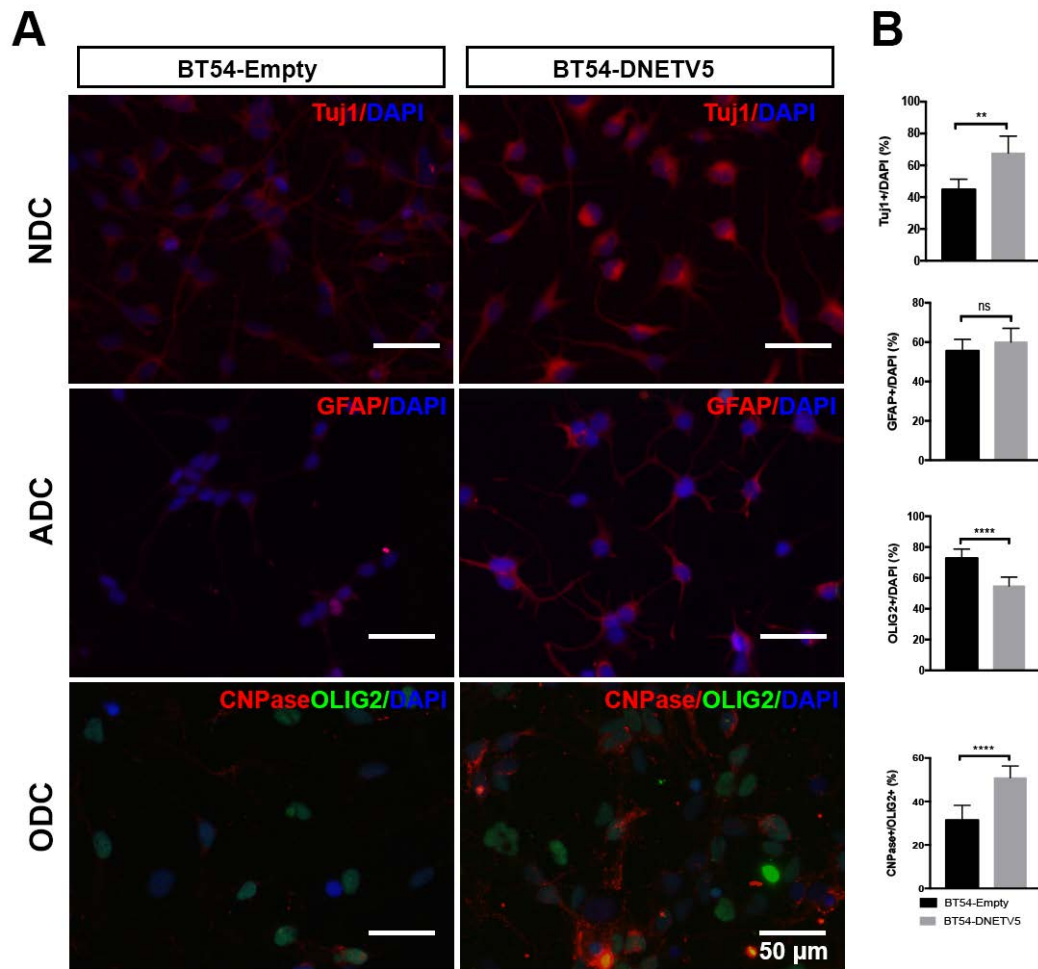
Figure S6: Etv5 inhibition in the ODG cell line BT-54 increases responsiveness to cues for neuronal and oligodendrocytic differentiation. Representative images showing the immunolabelling of BT54-DNETV5 and BT54 control cell lines with neural lineage markers (A). Quantification of the immunostained cells using lineage marker expression. BT54-DNETV5 cells differentiate into neurons with higher efficiency than control BT54 cells under the same differentiation conditions. There was no significant difference in astrocyte numbers under astrocytic differentiation condition between the BT54-DNETV5 and BT54 control line. BT54-DNETV5 cells undergo terminal oligodendrocyte differentiation and become mature oligodendrocyte with higher efficiency than BT54 controls under oligodendrocytic differentiating condition (B). ns – not significant, ** $p < 0.01$, **** $p < 0.0001$.

SUPPLEMENTARY METHODS

The Cancer Genome Atlas data analysis

The Cancer Genome Atlas (TCGA) Lower Grade Glioma (LGG) dataset was downloaded from the online UCSC Xena browser (https://xenabrowser.net/). Tumors that were histologically diagnosed as ODG (grade II or III) or oligoastrocytoma (OA) (grade II or III) that had IDH1 or IDH2 mutations and evidence of 1p19q codeletion (copy number log2(tumor/normal) ≤ -0.5) were included in our analyses. Etv1/4/5 gene expression levels were compared between ODG with wildtype *vs.* mutant CIC.

Immunofluorescence quantitation of neural lineages for presence or absence of CIC expression

A fixed number of Neurons (NeuN+), Astrocytes (GFAP+) and Oligodendrocytes (Olig2+) cells in mice brain sections were counted for the presence or absence of CIC expression. The percentages of CIC+ and CIC- cells in each lineage was ploted on a bar graph.

Alamar Viability assay

10% Alamar Blue reagent (Life Technologies, DAL1100) was added to cells in 96-well plates and allowed to incubate at 37ºC for 6 hours. The fluorescence reading from each well was then assessed ($\lambda_{ex/em}$: 544 nm/590 nm) using a SpectraMax M2^e microplate reader (Molecular Devices).

Antibodies

Primary antibodies directed against the following were used: CIC (1:500 IF, 1:1000 WB; A301-204, Bethyl), Olig2 (1:250 IF, 1:1000 WB, MABN50, Millipore), Olig2 (1:500, AB9610MI, Millipore), ETV1 (SAB1403794, Sigma), ETV4 (1:2000 WB, LS-C98380, LS BioSciences), ETV4 (1:500 IF 1:2000 WB, ARP32263_P050, AVIVA Systems Biology), ETV5 (1:1000 WB; sc-22807, Santa Cruz), ETV5 (1:500 IF, 1:2000 WB, 13011-1-AP, ProteinTech), GFP (1:500 IF; A11122, Thermo), GFP (1:250 AF, ab38689, Abcam), SOX2 (1:500 IF, ab92494, Abcam), Turbo-GFP (1:500 IF, OTI2H8, Origene), SOX2 (1:500 IF, 1:1000 WB, #3728, Cell Signalling), SOX9 (1:500 IF, ab76997, Millipore), SOX9 (1:250 IF,1:1000 WB, AB5535, Millipore), PDGFRA (1:500 IF, 1:1000 WB, 3174S, Cell Signalling), PDGFRA (1:250 IF, AF1062, R&D), CC1 (1:500 IF, OP80, Millipore), MBP (1:500 IF, ab40390, Abcam), Nestin (1:500 IF, 1:1000 WB, MAB353, Millipore), Tbr1 (1:500 IF, AB2261, Millipore), Tbr2 (1:500 IF, AB15894, Millipore), Tuj1 (1:500 IF, 1:1000 WB, MAB1195, R&D), GFAP (1:800 IF, 1:1000 WB, MAB360, Millipore), GFAP (1:500 IF, 345860, Calbiochem), ALDH1 (1:250 IF, ab87117, Abcam), NeuN (1:500 IF, MAB377, Millipore), Cre (1:500 IF, 1:2000 WB, NB100-5613, Novus), Ki67 (1:200; ab15580, Abcam), EdU (61135-33-9, Carbosynth US LLC). For routine immunofluorescence, secondary antibodies were: Alexa Fluor-488, -594 and -633) conjugated species-specific antibodies (Thermo) were used at 1:500 dilution. For the OPAL method (OPAL 4-color kit, Perkin Elmer), secondary antibodies used were anti-mouse HRP polymer (DAKO) and anti-rabbit HRP polymer (DAKO).

SUPPLEMENTARY REFERENCES

1. An RNA-Seq transcriptome and splicing database of glia, neurons, and vascular cells of the cerebral cortex. *Journal of Neuroscience*. 2014.